Modeling the Structure-Property Relationships of Nanoneedles: A Journey Toward Nanomedicine

ALBERT POATER,[1,2] ANA GALLEGOS SALINER,[2,3] RAMON CARBÓ-DORCA,[3] JORDI POATER,[3] MIQUEL SOLÀ,[3] LUIGI CAVALLO,[1] ANDREW P. WORTH[2]

[1]*Dipartimento di Chimica, Università di Salerno, Via Ponte don Melillo, I-84084 Fisciano (SA), Italy*

[2]*European Chemicals Bureau (ECB), Institute for Health and Consumer Protection, Joint Research Centre - European Commission, Via Enrico Fermi 2749, I-21027 Ispra (VA), Italy*

[3]*Institut de Química Computacional, Departament de Química, Universitat de Girona, Campus de Montilivi, E-17071 Girona, Catalonia, Spain*

Received 3 February 2008; Revised 7 April 2008; Accepted 28 April 2008
DOI 10.1002/jcc.21041
Published online 9 July 2008 in Wiley InterScience (www.interscience.wiley.com).

Abstract: Innovative biomedical techniques operational at the nanoscale level are being developed in therapeutics, including advanced drug delivery systems and targeted nanotherapy. Ultrathin needles provide a low invasive and highly selective means for molecular delivery and cell manipulation. This article studies the geometry and the stability of a family of packed carbon nanoneedles (CNNs) formed by units of 4, 6, and 8 carbons, by using quantum chemistry computational modeling methods. At the limit of infinite-length, these CNNs might act as semiconductors, especially when the number of terminal units is increased. CNNs are also potentially able to stabilize ions around their structure. Therefore, due to the apolar characteristics of CNNs and their ability to carry ionic species, they would be suitable to act as drug carriers through nonpolar biologic media.

 J Comput Chem 30: 275–284, 2009

Key words: carbon nanoneedle; nanomedicine; structure-property relationships; computational modeling; chemical hardness; electrophilicity

Introduction

Nanotechnology is an emerging science becoming increasingly important with many applications in a wide range of fields.[1] Manufactured nanoparticles (i.e., particles with at least one dimension below 100 nm) usually have unique properties[2] that make them very useful for commercial, technological, and therapeutic applications. However, nanotechnologies are still in an early stage of development and many research efforts are directed to the understanding of properties and behavior of nanomaterials, including nanoparticles (NPs). In particular, the current understanding of the toxicity of NPs is still rather limited and data on their behavior (e.g., mechanisms and pathways of toxicity, human exposure routes, physicochemical and biological properties relevant for modeling toxicity and adverse effects) are still relatively sparse. Some current efforts have been focused in theoretical modeling of NPs[3,4] and in the prediction of toxicological properties by using computational techniques.[5]

Special attention is paid to the biomedical and biotechnology applications of nanotechnology to nanomedicine[6] and in particular to medical diagnostics and imaging,[7] and to nanoneurosurgery.[8] Innovative techniques operational at the nanoscale level are being developed in therapeutic modalities, including advanced selective drug delivery systems and targeted nanotherapy.[9] Some of these modalities include polymeric NPs,[10] micelles,[11] liposomes and dendrimers,[7] fullerenes,[12,13] hydrogels,[14] nanoshells,[15] and smart surfaces. Some of the key performance characteristics of these materials are the high loading capacity, release kinetics, circulation time, biodistribution, size distribution, and stability.[16]

Ultrafine Nanoneedles

In this context, ultrathin needles[17] provide a low invasive means for molecular delivery, manipulating cells, and transferring genes in living cells by using atomic force microscopes.[18] DNA can be immobilized on the surface of nanoneedles by covalent

Additional Supporting Information may be found in the online version of this article.

Correspondence to: A. Poater; e-mail: albertpo@iqc.udg.es

bonding and affinity binding. This technique enables accurate displacement and low invasiveness.

Some studies have recently demonstrated that chemically modified carbon nanotubes can act as nanoneedles easily crossing biological barriers and penetrating a variety of cell types.[19–21] This finding opens the potential of functionalized carbon nanotubes as a new form of direct drug delivery.[22] These functionalized nanotubes capable of acting as cell-penetrating materials can behave as nanoneedles that pierce plasma membranes and translocate directly into cytoplasm without causing cell damage, with the advantage of being quickly excreted. The nanotubes also offer a structural advantage in that they are extremely thin but very long, offering a large surface area on which the required drug can be bound. This allows the amount of drug loaded onto the nanotube to be regulated. However, the mechanisms of action are still unclear and the release of the chemically conjugated drug from the nanoneedle is not always possible. Current investigations are directed to the study of increased efficiency of drug delivery and drug targeting,[23] improved release profiles and reversible associations for the intracellular release of the drug.[24]

In contrast, synthetic nanoneedles have been applied in oncology therapy[7] as highly selective ion channels that control the molecular traffic across the cell membrane, targeting specific diseased cells.[25] Similarly, magnetic drug targeting employing iron oxide nanoparticles as carriers is a promising cancer treatment avoiding side effects of conventional chemotherapy.[26] Once the drug is delivered, it can be easily eluted by simply changing either the ionic strength or the pH.

Recently, electronic and theoretical properties of ultrathin carbon[27] and nitrogen[28] needle-like and tube-like nanostructures, which are tighter than the smallest single wall nanotubes, have been studied by using quantum chemical calculations. Knowing that the synthesis of these structures is not relatively easy,[29] this article aims to study the geometry and stability of a family of packed carbon nanoneedles (CNNs) by using quantum chemistry computational modeling methods.

Computational Details

Chemical Structures

A family of packed CNNs was investigated using various terminal units (**C4**, **C6**, and **C8**) and a different number of layers (from 1 to 10 layers, and additional calculations with 15, 20, and 25 layers). Figure 1 displays these highly symmetrical structures corresponding to 10 layers.

Computational Calculations

All geometry optimization calculations have been performed at the B3LYP level, using the standard 6-31G(d) basis set with the Gaussian03 package,[30] that reveals to be a good computational method for nanoneedles.[27,28] The geometry optimizations were performed without symmetry constraints, and the nature of the minima was checked by analytical frequency calculations.

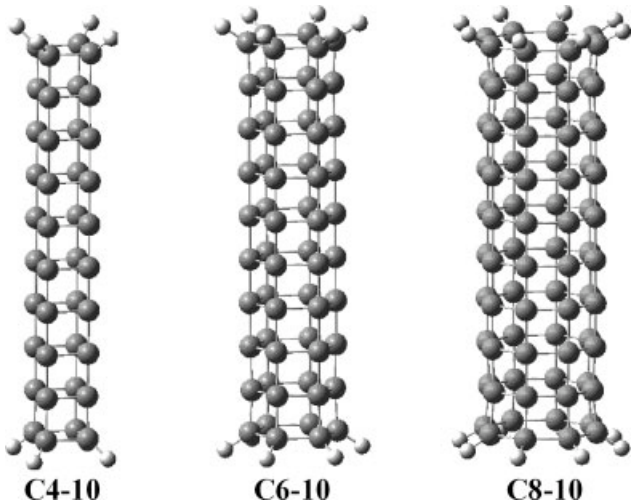

Figure 1. Structure of **C4**, **C6**, and **C8** CNNs with 4, 6, and 8 terminal units, respectively, and 10 layers.

Reactivity Descriptors

The chemical potential and molecular hardness for the N-electron system with total energy E and external potential $v(\vec{r})$ are defined as the following first and second derivatives of the energy with respect to N:[31,32]

$$\mu = \left(\frac{\partial E}{\partial N}\right)_{v(\vec{r})} = -\chi \tag{1}$$

and

$$\eta = \frac{1}{2}\left(\frac{\partial^2 E}{\partial N^2}\right)_{v(\vec{r})} = \frac{1}{2}\left(\frac{\partial \mu}{\partial N}\right)_{v(\vec{r})} \tag{2}$$

where χ in eq. (1) is the electronegativity. In numerical applications, μ and η are calculated using the finite difference approximation:

$$\mu \approx -\frac{1}{2}(\mathrm{IP} + \mathrm{EA}) \tag{3}$$

and

$$\eta \approx \frac{1}{2}(\mathrm{IP} - \mathrm{EA}) \tag{4}$$

The vertical ionization potential (IP) and the electron affinity (EA) can be obtained from the energy of the neutral, anionic, and the cationic species at the geometry of the corresponding N-electron neutral species, as follows:

$$\mathrm{IP} = [E(N-1) - E(N)] \tag{5}$$

$$\mathrm{EA} = [E(N) - E(N+1)] \tag{6}$$

Equations 3 and 4 can be simplified by using the Koopmans' theorem,[33] which approximates the electronic affinity and the ionization potential to the negative of the lowest unoccupied

Table 1. Calculated C−C Bond Distances and Average C−C Bond Distance ($\overline{d(C-C)}$) Between Layers (Å).

		d ($C_{layer\ (i)}$−$C_{layer\ (i+1)}$)									
	Layers	d (C_{layer1}−C_{layer2})	d (C_{layer2}−C_{layer3})	d (C_{layer3}−C_{layer4})	d (C_{layer4}−C_{layer5})	d (C_{layer5}−C_{layer6})	d (C_{layer6}−C_{layer7})	d (C_{layer7}−C_{layer8})	d (C_{layer8}−C_{layer9})	d (C_{layer9}−$C_{layer10}$)	$\overline{d(C-C)}$
C4	2	1.571									1.571
	3	1.587	1.587								1.587
	4	1.592	1.630	1.592							1.604
	5	1.589	1.627	1.627	1.589						1.608
	6	1.589	1.622	1.625	1.622	1.589					1.610
	7	1.589	1.623	1.621	1.621	1.623	1.589				1.611
	8	1.589	1.623	1.622	1.616	1.622	1.623	1.589			1.612
	9	1.588	1.622	1.622	1.617	1.617	1.622	1.622	1.588		1.612
	10	1.589	1.622	1.622	1.617	1.618	1.617	1.622	1.622	1.589	1.613
C6	2	1.565									1.565
	3	1.577	1.577								1.577
	4	1.582	1.632	1.582							1.599
	5	1.581	1.627	1.627	1.581						1.604
	6	1.579	1.621	1.624	1.621	1.579					1.605
	7	1.581	1.623	1.618	1.618	1.623	1.581				1.607
	8	1.580	1.623	1.621	1.612	1.621	1.623	1.580			1.609
	9	1.580	1.622	1.621	1.615	1.615	1.621	1.622	1.580		1.609
	10	1.580	1.622	1.620	1.615	1.617	1.615	1.620	1.622	1.580	1.610
C8	2	1.564									1.564
	3	1.570	1.570								1.570
	4	1.575	1.637	1.575							1.596
	5	1.575	1.635	1.635	1.575						1.605
	6	1.575	1.627	1.631	1.627	1.575					1.607
	7	1.574	1.629	1.622	1.622	1.629	1.574				1.608
	8	1.574	1.629	1.627	1.614	1.627	1.629	1.574			1.611
	9	1.574	1.628	1.626	1.618	1.618	1.626	1.628	1.574		1.612
	10	1.574	1.628	1.626	1.618	1.622	1.618	1.626	1.628	1.574	1.613

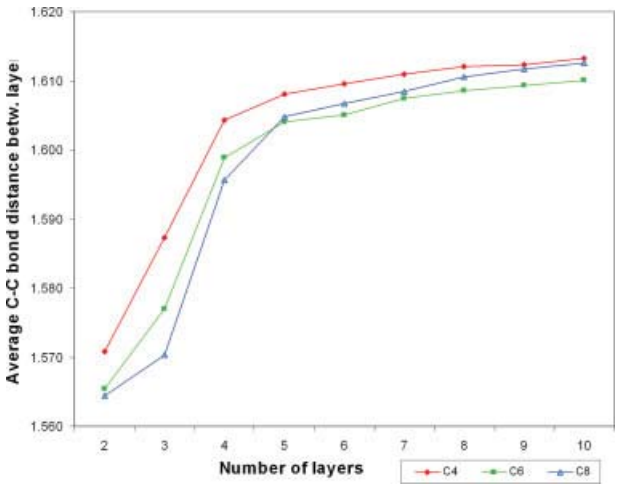

Figure 2. Calculated average C—C bond distance between layers *versus* number of layers for **C4** (red diamond), **C6** (green square), and **C8** (blue triangle) CNNs.

molecular orbital (LUMO) energy (ε_L) and the highest occupied molecular orbital (HOMO) energy (ε_H), respectively.

$$\mu \cong \frac{1}{2}(\varepsilon_L + \varepsilon_H) \tag{7}$$

and

$$\eta \cong \frac{1}{2}(\varepsilon_L - \varepsilon_H) \tag{8}$$

The electrophilicity index is defined as[34]:

$$\omega = \frac{\mu^2}{2\eta} \tag{9}$$

Results

Bond Distances and Stability

The electronic properties and energetic stability of the geometrical structures described above were investigated. Table 1 collects the C—C bond distances between layers and the corresponding average C—C bond distance ($\overline{d(C-C)}$) for each structure. The average C—C bond distance clearly reflects that when increasing the number of layers the strength between layers is lower, going from 1.571 to 1.613 Å for **C4**, from 1.565 to 1.610 Å for **C6**, and from 1.564 to 1.613 Å for **C8**. Geometrical differences between **C4**, **C6**, and **C8** are scarce and there is the trend of slightly shorter C—C distances between layers when increasing the number of terminal units. For **C4**, the study has been enlarged with additional calculations for 15, 20, and 25 layers. The longer CNNs have average C—C bond distances of 1.614 Å for **C4-15**, 1.615 Å for **C4-20**, and 1.616 Å for **C4-25**. These values are very similar with respect to **C4-10**, but they show a slight decrease of the C—C strength between layers, as already discussed (*vide supra*). This confirms the validity of the extrapolation from simplified CNNs to explain the properties of real CNNs at the limit of infinite length. Another characteristic is that, apart from the three external C—C bond distances between layers, the other C—C bond distances are very similar, with variations in a range of less than 0.002 Å.

Figure 2 clearly reflects the asymptotic trend of the C—C average bond distance. Differences of this average distance tend to be irrelevant after more than four layers are studied. When the number of layers increases, the C—C bond length between layers is shorter in both extremes of the needle, going from the 1.571 Å for **C4-2** to 1.589 Å for **C4-10**. And then the following distance between layers is commonly the largest, i.e., the distances between the second and the third layer, being the structures with six layers the unique exception, but with only a slight dif-

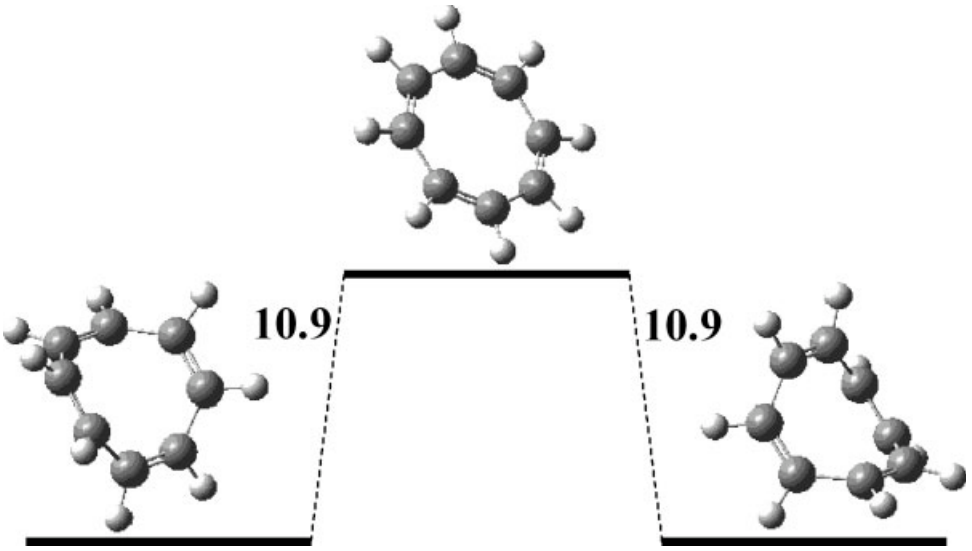

Figure 3. Interconversion of **C8-1** from both minima with S_4 geometry overcoming the transition state with D_{8h} geometry.

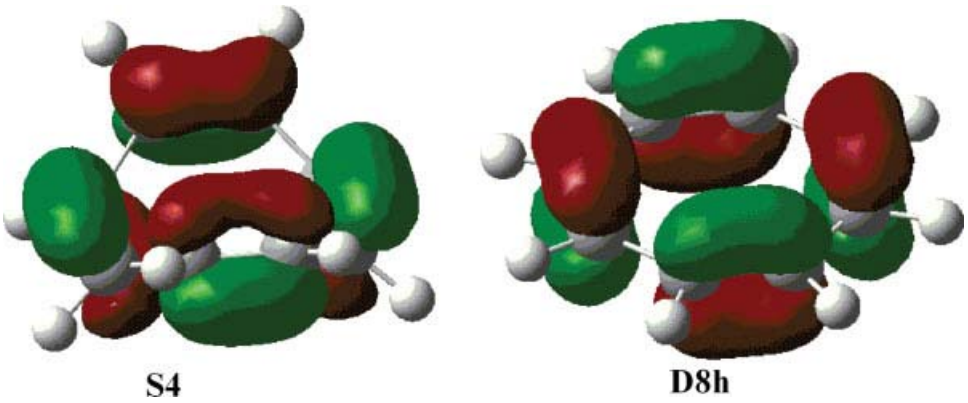

Figure 4. HOMO orbitals of the S_4 and D_{8h} geometrics of **C8-1**.

ference with respect to the central C—C distance that is the largest one.

When increasing the number of ring atoms that belong to a layer, the stability of the planar structure within one layer decreases. As previously described, it is especially dramatic for the **C8** structure, for which the D_{8h} conformation does not exist as a minimum, thus being a transition state that links the two identical conformations with S_4 geometry as displayed in Figure 3.

The impossible planarity of the minimum for **C8-1** is confirmed by the 9.9 kcal mol^{-1} (10.9 kcal mol^{-1} in Gibbs energy) between the S_4 isomer and the planar D_{8h} isomer that corresponds to the transition state that links both identical S_4 isomers displayed in Figure 3. A plausible explanation of the nonplanarity of **C8-1** is found by means of the Molecular Orbital Theory.[35,36] HOMO orbitals displayed in Figure 4 of the S_4 and D_{8h} geometries reveal that the S_4 conformation allows a stabilization of 13.9 kcal mol^{-1} with respect to the D_{8h} conformation, due to the accommodation of the antibonding character of the π orbitals involved.

Electronic Properties

As in previous papers,[37] conceptual DFT turns out to be a useful tool to compare the similarity and relationships between structures.[38,39] The calculated values of the HOMO-LUMO energy gap ($E_{HOMO\text{-}LUMO}$), chemical potential (μ), chemical hardness (η), and Parr electrophilicity (ω) for **C4**, **C6**, and **C8** CNNs have been collected in Table S1, for the different number of layers (N_{layers}). The $E_{HOMO\text{-}LUMO}$ gap decreases when increasing the number of layers. Although the single-layer compound clearly presents a different behavior because it cannot be considered a CNN, it is shown for comparison and to give an insight into the properties of the CNNs. With 10 layers the HOMO-LUMO has decreased significantly and reaches very small values, especially for the **C8-10** structures, where the gap is only

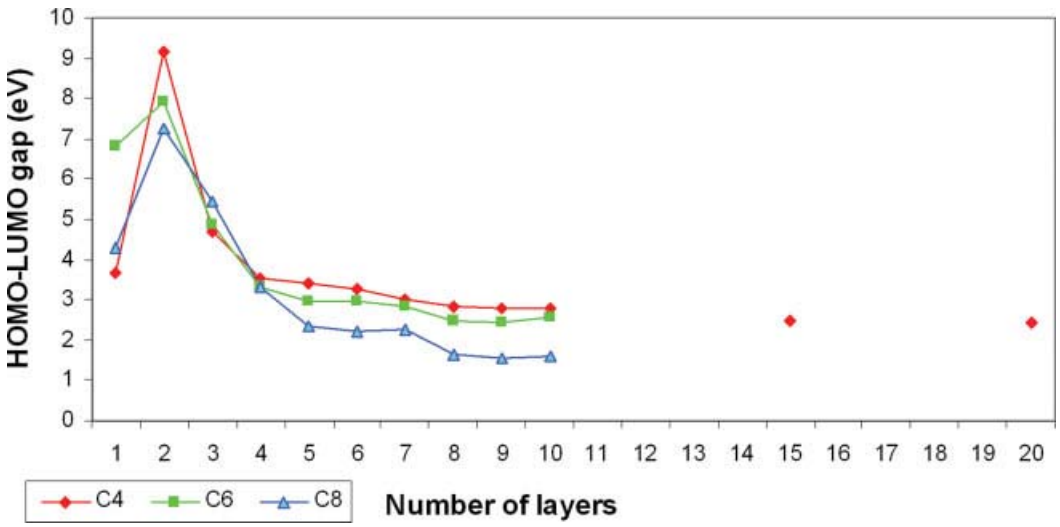

Figure 5. HOMO-LUMO energy gap *versus* number of layers for **C4** (red diamond), **C6** (green square), and **C8** (blue triangle) CNNs.

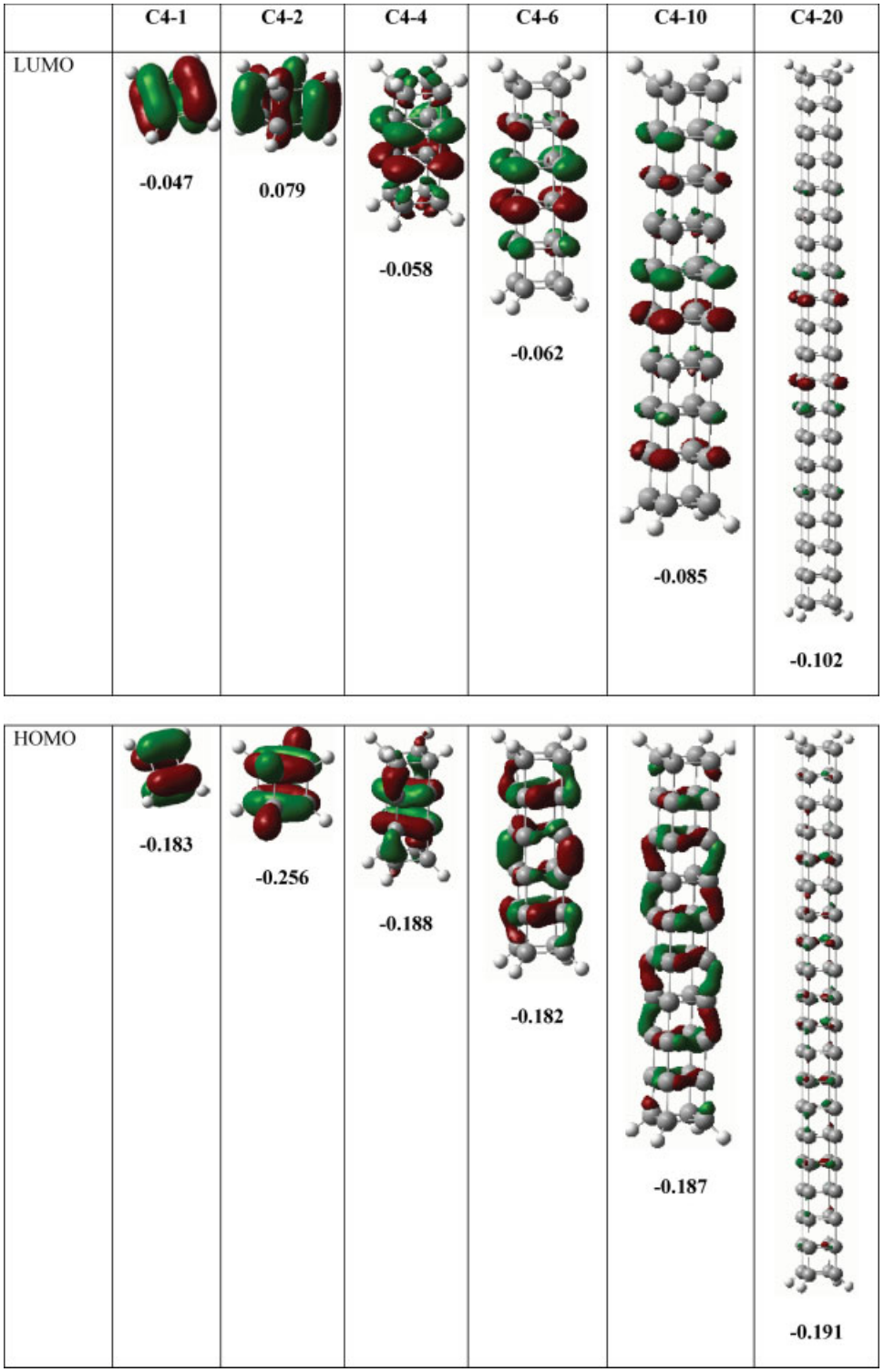

Figure 6. LUMO, degenerated HOMO and HOMO-1, and degenerated HOMO-2 and HOMO-3 orbitals for **C4** with 1, 2, 4, 6, 10, and 20 layers. [Color figure can be viewed in the online issue, which is available at www. interscience.wiley.com.]

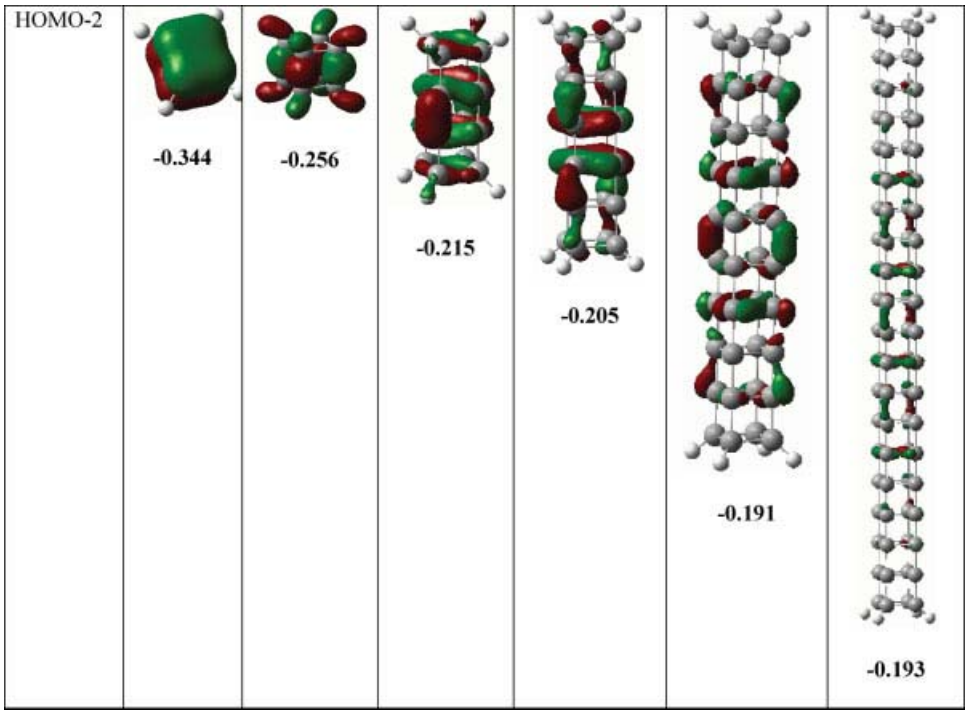

Figure 6. (*continued*)

1.574 eV with respect to the 2.771 eV of the **C4-10** structure. The **C4-15**, **C4-20**, and **C4-25** CNNs give values of 2.482, 2.437, and 2.358 eV, respectively. This reflects the same tendency for increasing number of layers but the decrease of the gap is smaller, as can be seen in Figure 5. The asymptotic value of the HOMO-LUMO gap might be too large to allow conductivity, thus agreeing with the paper of Wang and Mezey.[27] However, this asymptotic value is quite small at infinite length of the nanoneedle, pointing toward a certain semiconductor character when increasing the CNN size. Therefore, for very long layered structures CNNs, the corresponding CNNs are likely to have semiconducting properties and could possibly be used as actual semiconductors as the (3, 0) structures described by Wang and Mezey.[27]

When orbitals are displayed, it is possible to observe that the possible conjugation between layers for the shortest CNNs (from 1 to 4 layers) decreases with increasing number of layers. Figure 6 shows the comparison between the main orbitals of **C4-4**, **C4-10**, and **C4-20**. The strong overlaps both between layers and within layers present especially in **C4-4** nearly disappear in

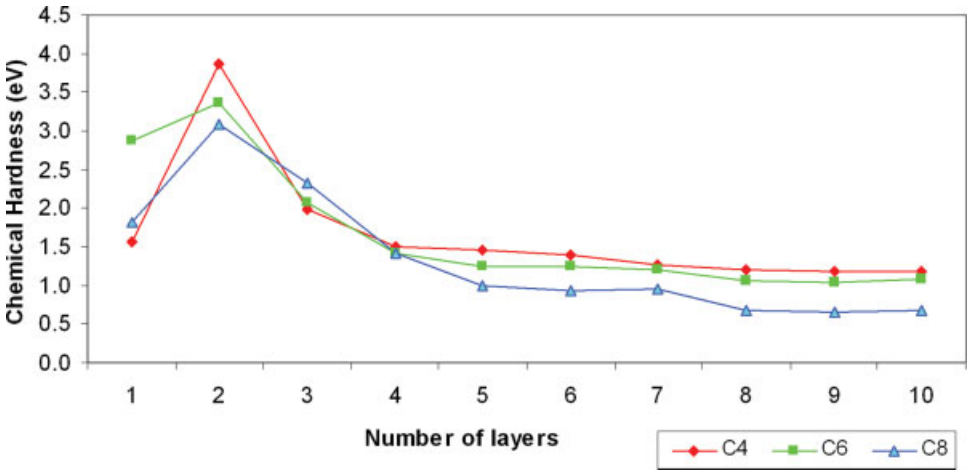

Figure 7. Chemical Hardness (eV) versus number of layers for **C4** (red diamond), **C6** (green square), and **C8** (blue triangle) CNNs. [Color figure can be viewed in the online issue, which is available at www.interscience.wiley.com.]

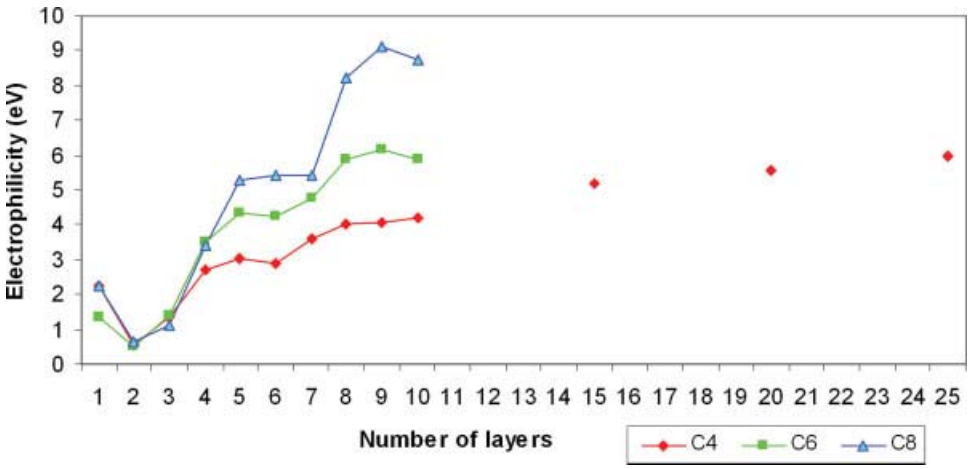

Figure 8. Electrophilicity versus number of layers for **C4** (red diamond), **C6** (green square), and **C8** (blue triangle) CNNs. [Color figure can be viewed in the online issue, which is available at www.interscience.wiley.com.]

C4-20. Therefore at infinite length the CNN properties cannot be extrapolated from the shortest structures. However, the pair HOMO and HOMO-1 and also the pair HOMO-2 and HOMO-3 are degenerated in all the studied CNNs, despite increasing the length of the needle, except for the CNNs with one or two layers that have a different behavior from the rest of the series. The orbitals for the **C4** CNNs are similar to **C6** and **C8** ones (see supporting information for complete series of orbitals).

Bearing in mind that electronegativity is obtained through chemical potential, it is possible to observe that increasing the number of layers increases electronegativity of the needle. However, if **C4**, **C6,** and **C8** are compared, there is no clear trend, with **C6** being the most electronegative structure, and then **C8** more electronegative than **C4** for more than 3 layers. When the number of layers is small, such trends do not hold, which is why a relatively large number of layers was modeled. Therefore, in spite of the fact that **C8** presents slightly lower values of electronegativity than **C6,** in general terms the larger the width of the CNN, the larger the electronic movement described by the chemical potential (μ) is, at least when comparing **C6** or **C8** with respect to **C4**. Furthermore **C4-25** presents a μ value of 3.482, thus reinforcing the idea that at infinite length these CNNs will have a semiconductor behavior.

The chemical hardness for **C8-1** with D_{8h} geometry is 1.820, compared to the 1.022 for the S_4 geometry, in line with the instability of the planar minimum. The trend is clear observing Figure 7, when increasing the number of layers the CNN is less and less hard, and when going from **C4** to **C6** and **C8** the CNN is even less hard. In the case of the least hard **C8**, these structures are more reactive with respect to other chemical species.

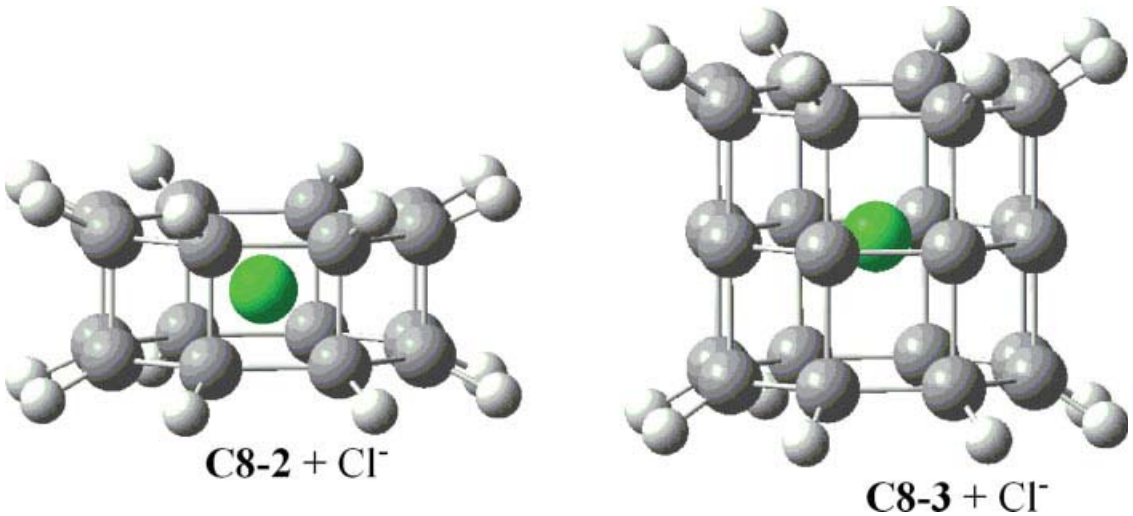

Figure 9. C8-2 and **C8-3** structures as carriers of one chloride anion. [Color figure can be viewed in the online issue, which is available at www.interscience.wiley.com.]

The values for the **C4** CNNs with 15, 20, and 25 layers are 1.052, 1.032, and 0.999 showing the same decreasing trend, but not enough to predict very instable species at an infinite length. This confirms the structural factor that describes a slightly lower binding strength between layers when increasing the number of layers of the CNN.

The Parr electrophilicity (ω) is higher when the number of layers is increased, and furthermore **C8** CNNs are much more electrophilic than the **C4** and **C6** CNNs for more than 4 layers. Figure 8 illustrates that the expected asymptotic behavior described by Wang and Mezey[27] that precludes conductivity for these CNNs at the infinite length is not completely true. Instead of this asymptotic behavior a quite linear relationship between the electrophilicity and the increase of the number of layers is observed, although with a low slope. Therefore, it is plausible that at infinite length the synthesized species would be quite electrophilic, as observed in Figure 8.

Utilities

The extraordinary properties of CNNs make them potentially suitable in the biological field. According to the first computational attempt to model CNNs, they have been found to be potentially good carriers. Taking advantage of the unexpected high electrophilicity for **C8** structures, an attempt to simulate the application of CNNs has been made including charged ions inside their structure. This is possible because they can accommodate ions in the middle of each layer and also between layers. The first approach reveals that including a chloride anion inside the **C8-2** and **C8-3** structures decreases the HOMO-LUMO gap from 7.265 to 5.438 and from 5,462 to 0.402 eV, respectively. Figure 9 shows that the chloride in **C8-2** is between the layers and for **C8-3** within the layers, in the middle of the central layer of the CNN. Therefore it seems quite reasonable that CNNs including the carried ions could adopt the property of conductivity which would have potential applications in facilitating ion exchange in cells. On the other hand, potassium cations have provided also a decrease of the HOMO-LUMO gap from 5.462 to 4.329 for **C8-3** structure, although the increase of conductivity is lower than for the chloride anion because the electrophilicity of **C8** structures favor the interaction with anionic species. Current efforts are focused on other ions, especially iron, as well as in modifying the structure of the CNN in order to be able to accommodate larger ions, especially larger anions. More research is needed to tailor the use of CNNs to deliver drugs, to improve the release of the drugs, and to complement the theoretical studies with toxicity studies.

Conclusions

Different computational techniques have been applied to study theoretical physicochemical properties of carbon packed nanoneedles that can be directly related to reactivity, detailing how the different geometrical and reactivity measures build up a picture of how the properties of CNNs depend on length and diameter.

The versatility of CNNs as well as the possibility to control their length in terms of number of layers makes them potentially useful as specifically targeted drug delivery systems. However, more research on the assessment of potentially adverse human health effects should be conducted. For instance, the exposure to nanotube fibers has been associated with mesothelioma in a mouse model, pulmonary fibrosis, and lung cancer.[40]

The studied families of CNNs can be considered as carbon nanostructures with unique structural and chemical properties. Because of their unusual electronic properties, they have potential practical applications as nanomaterials and nanostructure devices. In addition, infinite-length CNNs are likely to have semiconducting properties, allowing their use as semiconductors in nanostructure devices. The increase of the diameter of the needle makes it more conductive. However, the main property of these CNNs is the role as biologic ion carriers. When the ring is made of at least eight atoms, it is possible to bind potassium, sodium, chloride, or iron ions that would enlarge this conductivity. More research is focused on this aspect, to explore the use of CNNs as a possible mechanism for the oral ingestion of ionically charged drugs embedded in the nonpolar CNNs, by varying the width of the cavity of the CNNs.

Acknowledgments

This research has been financed by the Spanish Ministry of Education and Culture (MEC) through projects CTQ2006-15634 and CTQ2005-08797-C02-01/BQU and through a contract with Basell Polyolefin. The authors thank the CINECA (INST grant) for financial support. A.G. is grateful for the allocation of a postdoctoral contract by DURSI of Generalitat de Catalunya. The authors also thank referees for their useful comments.

References

1. Ouyang, M.; Huang, J.-L.; Lieber, C. M. Acc Chem Res 2002, 35, 1018.
2. Ajayan, P. M. Chem Rev 1999, 99, 1787.
3. Tsakovska, I.; Saliner, A. G.; Bassan, A.; Worth, A. Computational modelling of nanoparticles. Poster presented at the 2nd Nanotoxicology Conference, Venice, April 19–21, 2007. Available at: http://www.informahealthcare.com/nanotoxicology/index.html and http://ecb.jrc.it/QSAR.
4. Poater, A.; Saliner, A. G.; Worth, A. Modelling NanoNeedles: A journey towards Nanomedicine. Poster presented at the 2nd Nanotoxicology Conference, Venice, April 19–21, 2007. Available at: http://www.informahealthcare.com/nanotoxicology/index.html and http://ecb.jrc.it/QSAR.
5. Worth, A.; Bassan, A.; Saliner, A. G.; Tsakovska, I. Towards in silico approaches for investigating the activity of nanoparticles. Communication presented at the 2nd Nanotoxicology Conference, Venice, April 19–21, 2007. Available at: http://www.informahealthcare.com/nanotoxicology/index.html and http://ecb.jrc.it/QSAR.
6. European Commission. European Technology Platform on Nano-Medicine, Vision Paper and Basis for a Strategic Research Agenda for NanoMedicine. European Commission: Brussels, 2005.
7. Portney, N. G.; Ozkan, M. Anal Bioanal Chem 2006, 384, 620.
8. Leary, S. P.; Liu, C. Y.; Apuzzo, M. L. Neurosurgery 2006, 58, 1009.
9. Kumar M. N. V. R. J Pharm Pharm Sci 2000, 3, 234.

10. Bergemann, C.; Müller-Schulte, D.; Oster, J.; à Brassard, L.; Lübbe, A. S. J Magn Mater 1999, 194, 45.
11. Kim, Y.; Dalhaimer, P.; Christian, D. A.; Discher, D. E. Nanotechnology 2005, 16, S484.
12. Gallo, M.; Favila, A.; Glossman-Mitnik, D. Chem Phys Lett 2007, 447, 105.
13. Simon, F.; Peterlik, H.; Pfeiffer, R.; Bernardi, J.; Kuzmany, H. Chem Phys Lett 2007, 445, 288.
14. Vinogradov, S. V.; Bronich, T. K.; Kabanov, A. V. Adv Drug Delivery Rev 2002, 54, 135.
15. Zahr, A. S.; de Villiers, M.; Pishko, M. V. Langmuir 2005, 21, 403.
16. Allen, C.; Maysinger, D.; Eisenberg, A. Colloids Surf B Biointerfaces 1999, 16, 3.
17. Bradley, D. Drug Discov Today 1997, 2, 452.
18. Obataya, I.; Nakamura, C.; Han, S. W.; Nakamura, N.; Miyake, J Nanobiotechnol 2005, 1, 347.
19. Lacerda, L.; Bianco, A.; Prato, M.; Kostarelos, K. Adv Drug Delivery Rev 2006, 58, 1460.
20. Klumpp, C.; Kostarelos, K.; Prato, M.; Bianco, A. Biochim Biophys Acta 2006, 1758, 404.
21. Kostarelos, K.; Lacerda, L.; Pastorin, G.; Wu, W.; Wieckowski, S.; Luangsivilay, J.; Godefroy, S.; Pantarotto, D.; Briand, J. P.; Muller, S.; Prato, M.; Bianco, A. Nat Nanotechnol 2007, 2, 108.
22. Prato, M.; Kostarelos, K.; Bianco, A. Acc Chem Res 2008, 41, 60.
23. Molema, G. Drug Targeting; Wiley-VCH Verlag GmbH : Weinheim, 2001; pp. 1–22.
24. Lin, C.-C.; Metters, A. T. Adv Drug Delivery Rev 2006, 58, 1379.
25. Hara, C.; Tateyama, K.; Okano, H.; Miyawaki, A. Neurosci Res 2007, 58, S242.
26. Alexiou, C.; Schmid, R. J.; Jurgons, R.; Kremer, M.; Wanner, G.; Bergemann, C.; Huenges, E.; Nawroth, T.; Arnold, W.; Parak, F.G. Eur Biophys J 2006, 35, 446.
27. Wang, J. L.; Mezey, P. G. J Chem Inf Model 2006, 46, 801.
28. Wang, J. L., Lushington, G. H., Mezey, P. G. J Chem Inf Model 2006, 46, 1965.
29. Alonso, M.; Poater, J.; Solà, M. Struct Chem 2007, 18, 773.
30. Frisch, M. J.; Trucks, G. W.; Schlegel, H. B.; Scuseria, G. E.; Robb, M. A.; Cheeseman, J. R.; Montgomery, J. A., Jr.; Vreven, T.; Kudin, K. N.; Burant, J. C.; Millam, J. M.; Iyengar, S. S.; Tomasi, J.; Barone, V.; Mennucci, B.; Cossi, M.; Scalmani, G.; Rega, N.; Petersson, G. A.; Nakatsuji, H.; Hada, M.; Ehara, M.; Toyota, K.; Fukuda, R.; Hasegawa, J.; Ishida, M.; Nakajima, T.; Honda, Y.; Kitao, O.; Nakai, H.; Klene, M.; Li, X.; Knox, J. E.; Hratchian, H. P.; Cross, J. B.; Bakken, V.; Adamo, C.; Jaramillo, J.; Gomperts, R.; Stratmann, R. E.; Yazyev, O.; Austin, A .J.; Cammi, R.; Pomelli, C.; Ochterski, J. W.; Ayala, P. Y.; Morokuma, K.; Voth, G. A.; Salvador, P.; Dannenberg, J. J.; Zakrzewski, V. G.; Dapprich, S.; Daniels, A. D.; Strain, M. C.; Farkas, O.; Malick, D. K.; Rabuck, A. D.; Raghavachari, K.; Foresman, J. B.; Ortiz, J. V.; Cui, Q.; Baboul, A. G.; Clifford, S.; Cioslowski, J.; Stefanov, B. B.; Liu, G.; Liashenko, A.; Piskorz, P.; Komaromi, I.; Martin, R. L.; Fox, D. J.; Keith, T.; Al-Laham, M. A.; Peng, C. Y.; Nanayakkara, A.; Challacombe, M.; Gill, P. M. W.; Johnson, B.; Chen, W.; Wong, M. W.; Gonzalez, C.; Pople, J. A. Gaussian 03; Gaussian: Wallingford, CT, 2004.
31. (a) Parr, R. G.; Donnelly, R. A.; Levy, M.; Palke, W. E. J Chem Phys 1978, 68, 3801; (b) Parr, R. G.; Pearson, R. G. J Am Chem Soc 1983, 105, 7512; (c) Parr, R. G.; Yang, W. Density Functional Theory of Atoms and Molecules; Oxford University Press: New York, 1989.
32. Pearson, R. G. Chemical Hardness: Applications from Molecules to Solids; Wiley-VCH: New York, 1997.
33. Koopmans, T. Physica (Utrecht) 1934, 1, 104.
34. Parr, R. G.; von Szentpaly, L.; Liu, S. J Am Chem Soc 1999, 121, 1922.
35. Hohenberg, P.; Kohn, W. Phys Rev 1964, 136, 864.
36. Kohn, W.; Sham, L. J Phys Rev A 1965, 140, 1133.
37. De Proft, F.; Van Alsenoy, C.; Peeters, A.; Langenaeker, W.; Geerlings, P. J Comput Chem 2002, 23, 1198.
38. Poater, A.; Jaque, P.; Toro-Labbé, A.; Solà, M. J Phys Chem B 2006, 110, 6526.
39. Costas, M.; Ribas, X.; Poater, A.; López Valbuena, J. M.; Xifra, R.; Company, A.; Duran, M.; Solà, M.; Llobet, A.; Corbella, Usón, M. A.; Mahía, J.; Solans, X.; Shan, X.; Benet-Buchholz, J. Inorg Chem 2006, 45, 3569.
40. Donaldson, K.; Aitken, R.; Tran, L.; Stone, V.; Duffin, R.; Forrest, G.; Alexander, A. Toxicol Sci 2006, 92, 5.